09

Pulsed tunable quantum cascade laser in the spectral range of 9.6−12.5 μm

© D.R. Anfimov, Ig.S. Golyak, P.P. Demkin, E.N. Zadorozhny, I.B. Vintaykin, A.N. Morozov, I.L. Fufurin

Bauman Moscow State Technical University,
105005 Moscow, Russia
e-mail: dimananfimov97@gmail.com

Received January 26, 2024
Revised January 26, 2024
Accepted January 26, 2024

A pulsed quantum cascade laser tunable in the spectral range of 9.6−12.5 μm is presented. The maximum pulse power is 199.8 mW, the maximum average power is 7.57 mW, the tuning step is 2 cm^{-1} and the spectral line width is 2 cm^{-1}. The schematic diagram of the quantum cascade laser, the main components and their technical characteristics are described. The quantum cascade laser, a multi-pass Herriott gas cell with an optical path length of 76 m, and two mercury-cadmium-telluride thermoelectrically cooled photodetectors comprise an experimental setup intended for gas absorption infrared spectroscopy. The transmission spectra measurements of an acetone mixture at 100 ppm concentration in nitrogen are reported.

Keywords: quantum cascade laser, Herriott gas cell, Littrow configuration, gas absorption spectroscopy, superlattice, quantum well.

DOI: 10.21883/0000000000

Introduction

A quantum cascade laser (QCL) is a unipolar laser that emits mainly in the infrared (IR) or terahertz range due to the electron transition between energy levels in quantum wells in the conduction band inside the active region [1]. The active region is a semiconductor heterostructure (superlattice), in which potential barriers alternate, for example from InAlAs, and quantum wells, for example from InGaAs [2,3]. Modern methods of growing heterostructures, such as molecular beam epitaxy, allow creating arbitrary structures for a specific application [4].

QCL have a high average radiation power at room temperature; a wide adjustment range (more than 900 cm^{-1}) with a tuning step of no more than 1 cm^{-1}, high energy efficiency (efficiency > 10%), compactness, reliability, stability [5]. All these properties allow the use of QCL in compact devices. There are various designs of the QCL resonator, such as the Fabry−Perot QCL that are multimode and at the same time have a higher output power [6], a distributed feedback laser (DFB) for single-mode operation [7] and QCL with an external cavity (EC) [8], where wavelength selection is usually carried out using an external diffraction grating (Littrow configuration).

QCL can be used to create technical tools for solving a wide range of applied problems in spectroscopy, safety, ecology and biomedicine [9]. The active use of QCL with a wide range of restructuring is presented by Block Engineering. This company presents on the market devices consisting of several „mini-QCL“ covering various spectral ranges, which are compact modules 1 cubic inch in size and the weight is 75 g. The width of the tuning range is more than 1100 cm^{-1} with an average output power of 0.5 to 15 mW [10].

The results of the identification of various chemical and explosive compounds [13] using diffuse reflectance spectroscopy are provided in Ref. [11,12]. The substance is located on various substrates, both natural and artificial, in a solid or liquid state. The laser radiation in the range 5−12 μm falls on the substance. The radiation reflected by the substance and the substrate is collected using focusing lenses on a Mercury Cadmium Telluride (MCT) photodetector cooled by a cascade of Peltier elements. Then the substances are identified by the reflectance spectrum [14,15].

The results of the detection of trace amounts of various chemicals, including explosives, using QCL with an external cavity in the range 7.7−11.8 μm are presented in Ref. [16–19]. The radiation moves along the plane, and using an IR camera with a spatial resolution of 70 μm, a hypercube with a size of 128 × 128 pixels and a depth of 130 wavelengths is filmed. Thanks to the high-speed camera, the hypercube is recorded in 0.1 s. The mass of 100 μg of caffeine was detected at a distance of 5 m [16], 100 μg of saccharin was detected at a distance of 25 m and trace amounts of pentaerythritol tetranitrate were detected at a distance of 0.1 m [19]. The detection limits of [17] for pentaerythritol tetranitrate were 6 ng per pixel. Mathematical methods for modeling hypercubes, which can be used to refine identification algorithms, are presented in Ref. [18]. The results of identification of biological objects on various surfaces, which demonstrates the possibility of creating a biological protection device based on QCL are presented in Ref. [10,20].

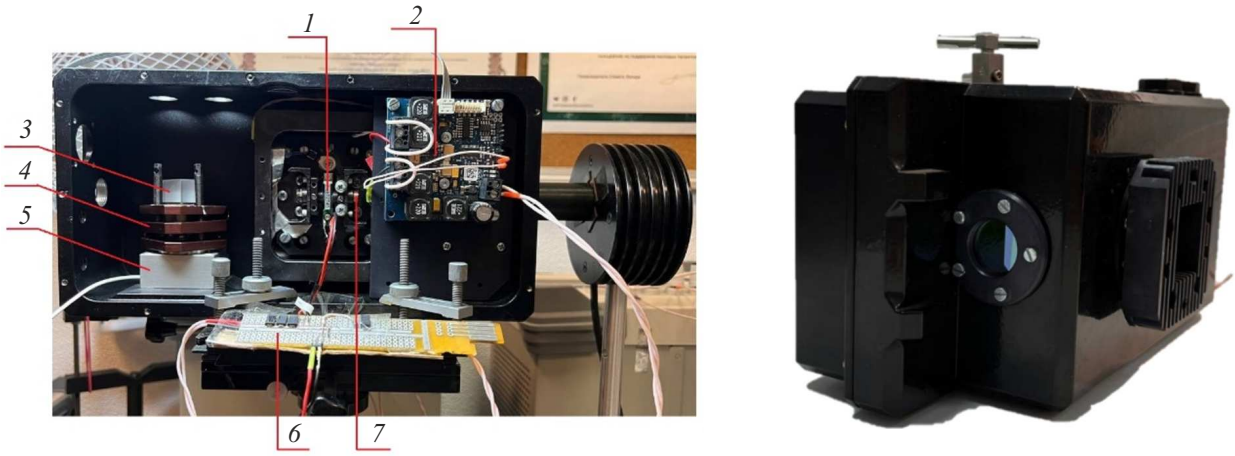

Figure 1. Appearance of the QCL. *1* — QCL chip; *2* — thermoelectric controller for controlling the Peltier element; *3* — diffraction grating; *4* — inclined platform; *5* — rotary motor; *6* — QCL chip control board; *7* — aspherical lens.

Diffuse reflectance spectroscopy is used to study biological tissues. This can help both in the development of non-invasive methods for the cancer cells analysis inside the human body [21,22], and for the skin lesions study [23].

There are also many studies of glucose in human blood *in vivo* using QCL [24]. Various QCL configurations are used for this purpose. A standard deviation of glucose concentration of 17.5 mg/dl was obtained by fiber laser spectroscopy using a distributed feedback laser with a wavenumber of 1031.0 cm^{-1} with a power of 1.0 mW and a pulse duration of 50 ns compared with glucose measurements *in vitro* [25]. A measurement error of 20 mg/dl [26] was obtained using a laser with an external cavity in the range 890–2020 cm^{-1} with a peak power of 500 mW and a pulse duration of 400 ns.

Infrared spectroscopy is one of the most common methods of studying protein reactions at the atomic level. The appearance of QCL allows for rapid monitoring of the reaction in the microsecond time domain, which could not be achieved using Fourier spectrometers [27]. QCL also have a higher power density and can be used to study wide protein layers [28].

Powerful lasers are of particular interest (with a power of 1 W). There are QCL with a wavelength of about 8 μm, presented in Ref. [29,30], as well as QCL with wavelength of about 8.5 μm [31].

Currently, one of the most effective methods of identifying gases along long paths is the use of FTIR spectrometers with which can be applied as safety equipment at facilities with a large number of people or at production sites [32,33]. As an alternative, the results of the identification of freon sprayed on a route with a length of 310 and 562 m using QCL are presented in Ref. [34]. The laser beam has a low divergence unlike broadband globars, which allows using a system of reflectors to realize an absolutely arbitrary beam movement inside an object to improve the quality of monitoring chemical contamination compared with FTIR spectrometers.

QCL makes it possible to identify a small amount of a substance (ppb units) in a wide spectral range, on which the number of identified substances depends. For example, the results of identification of 22 ppm acetone and 60 ppm ethanol in a gas cell with a size of 32.4 cm and an optical path length of 54.36 m are presented in Ref. [35]. 80 ppb of acetone and 100–120 ppb of ethanol and methanol were identified in Ref. [36] in a gas cell with an optical path length of 76 m using machine and deep learning methods. The results of the identification of multicomponent mixtures are also presented. Such setups can be used in environmental problems to locally determine the concentration of greenhouse gases such as CO, NO, NO_2, N_2O and SO_2 [37–39]. QCL are also used for identification of microplastics in water [40].

The results of measuring the concentration of acetone in exhaled breath in patients with type 1 diabetes are presented in Ref. [41]. The concentrations of this substance are extremely low (tens of ppb), but in experimental setups using a multi-pass gas cells [42,43] it is possible to determine various diseases due to the wide spectrum of QCL radiation and the use of modern signal processing methods [44–46].

This paper presents the scheme and technical characteristics of the developed QCL in the range from 9.6 to 12.5 μm based on a circuit with an external cavity (Littrow configuration), which allows for a wide range of tuning. The results of using QCL in an experimental setup for laser IR absorption spectroscopy of gas mixtures are presented.

1. QCL IR design

Figure 1 shows the appearance of the developed tunable QCL. Inside the QCL case there is a QCL chip with its own heat sink (Alpes Lasers, Switzerland), emitting in

Main QCL technical characteristics

Characteristic	Unit	Value
Tuning range	μm	9.6–12.5
Maximum average radiation Power	mW	7.57
Maximum pulse power	mW	199.8
Pulse duration of the emmiting radiation	ns	278
Pulse repetition rate	kHz	175.4
The distance between peaks	cm^{-1}	1.705 ± 1.085
Intensity peak width, not more than	cm^{-1}	2
Beam divergence, no more than	mrad	5
Beam shape at a distance of 530 mm	mm	Ellipse 3.5×5
Power consumption of the device from the mains 220 V 50 Hz	W	50
Overall dimensions length×width×height	mm	$130 \times 150 \times 250$
Weight	kg	6
QCL chip efficiency	%	12.6

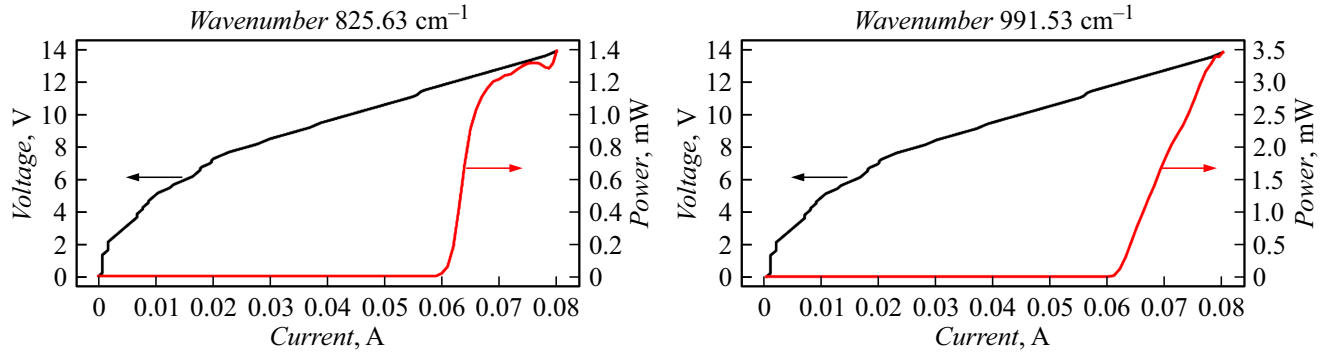

Figure 2. The volt-ampere characteristic (black) and average output power (red) QCL for wave numbers 825.63 and 991.53 cm^{-1}.

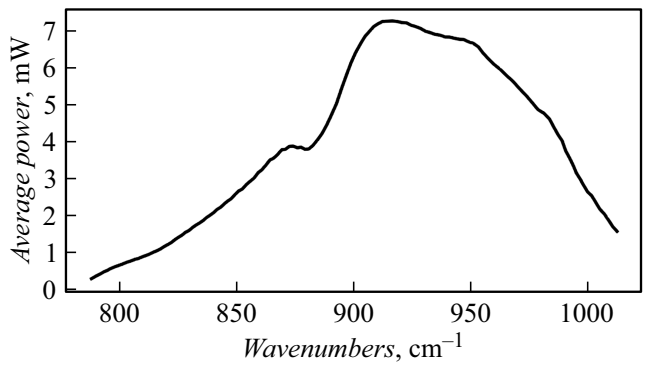

Figure 3. The spectrum of the average output power of QCL. Voltage 14 V, temperature 18°C.

the range 9.6–12.5 μm pos. 1. The external resonator contains two aspherical lenses *7*, located on both sides of the waveguide, with a refractive index 2.604 ± 0.003 and an effective focal length 1.87 ± 0.01 mm. The external resonator is built according to the Littrow configuration using a diffraction grating *3*, the operating range of which is from 9 to 11 μm. The reflective diffraction grating has 150 strokes per mm and a dispersion of 4.2 nm/mrad (Thorlabs, USA). The diffraction grating is located on an inclined platform *4* mounted on a rotary motor with an optical encoder *5*. The encoder resolution is 109 μrad, which allows positioning the diffraction grating with a minimum rotation angle of 125 μrad with an accuracy of 0.017%. The QCL chip is maintained at a constant temperature of 18°C using a Peltier element and a thermoelectric controller *2*, which allows maintaining the temperature with a maximum deviation of 0.001 K. The pulse voltage of 14 V with a pulse duration of 300 ns and a duty cycle of 5% on the laser chip is supported by a field MOSFET transistor *6*. The thermoelectric controller is controlled and pulses are generated using the STM32H743 microcontroller.

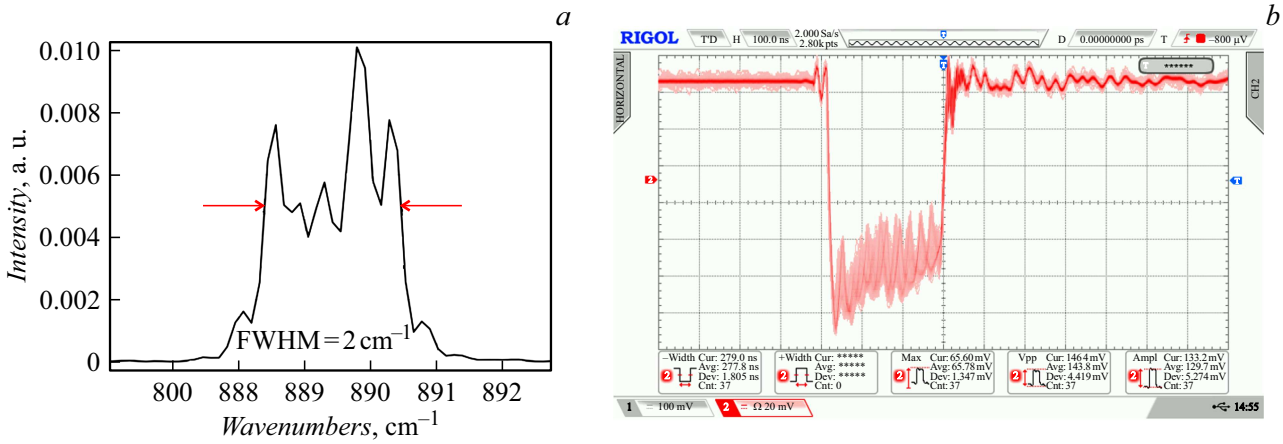

Figure 4. *a* — the spectral shape of the QCL pulse at the wavenumber 889 cm^{-1}. The spectrum line width is 2 cm^{-1}; *b* — the shape of the QCL radiation pulse on the MCT photo-receiving device.

The table shows the characteristics of the developed QCL. The maximum pulse power was calculated taking into account the shape of the pulse.

The volt-ampere characteristics (for the pulse voltage on the QCL chip) and the dependence of the average radiation power on the current for the developed QCL on two different wave numbers are presented in Figure 2. Figure 3 shows the spectrum of the average power of QCL.

Figure 4 shows the spectral shape of the pulse measured on the Thorlabs OSA207C Fourier spectrometer with a spectral resolution of 0.25 cm^{-1}, and the electrical shape of the pulse measured using a MCT photo-receiving device cooled by a cascade of Peltier elements.

The PVMI-4TE-10.6 photodetector (VIGO Photonics, Poland) is used as a Photodetector (PD) which consists of the following elements:

- MCT photodiode with active area 2 × 2 mm and lens;
- Murata NTC thermistor of type NCP03XM222E05RL;
- thermoelectric controller (TEC) with 4 cooling stages providing a temperature of 198 K.

TEC PD is designed to set and maintain the temperature of the photodiode at a predetermined level. It includes: a controlled step-down pulse converter, an automatic control system and a monitoring system for temperature, error voltage and energy parameters — voltage, current and power at the input and output of the controller. The data is transmitted to the control and processing unit via the interface I^2C.

The PD amplifier consists of: a transimpedance amplifier that converts the photodiode current into voltage (relative to ground); a differential amplifier that converts the common-mode signal of a transimpedance amplifier into a differential one; a modulator that reverses the polarity of the input signal; a differential integrator, with reset; a 24-bit sequential approximation ADC with a differential input; a comparator that triggers at the front and back of the input signal, which will allow the control unit to determine the time parameters of the pulses. The detector amplifier is connected to the control and processing unit via a high-speed LVDS interface.

2. Application of QCL

The experimental setup for laser IR absorption spectroscopy of gas mixtures, including exhaled breath is shown in Fig. 5. The multi-pass Herriott gas cell *6* with an optical path length of 76 m receives a gas mixture using a pump *1*. The radiation from QCL *2*, falling on the beam splitter *3*, is separated, and part of the radiation falls on the reference photodetector *4*, and the other part passes through the gas cell and falls on the signal photodetector *5*.

The main characteristics of the above experimental setup, as well as the calculation of the maximum detectable concentrations for various chemicals are presented in Ref. [46].

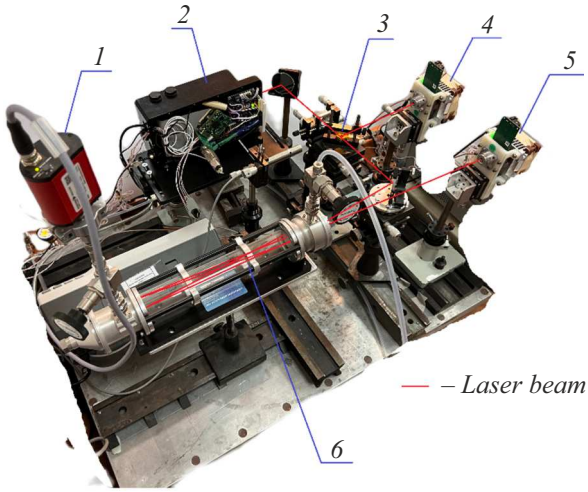

Figure 5. An experimental setup for the gas mixture analysis. *1* — pump, *2* — QCL, *3* — beam splitter plate, *4* — reference photodetector, *5* — signal photodetector, *6* — Herriott multi-pass gas cell.

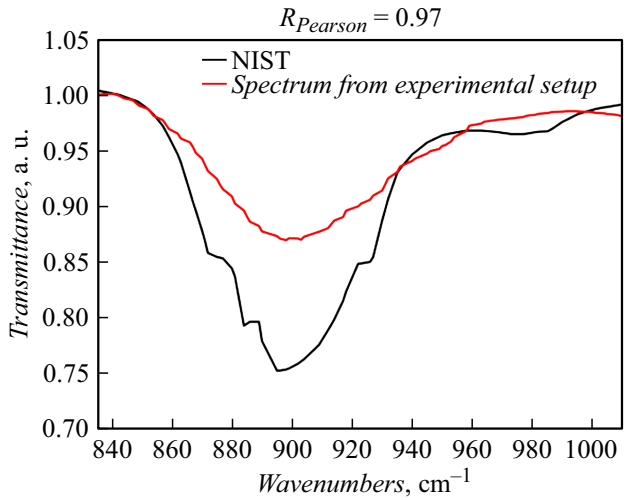

Figure 6. The transmission spectrum of 100 ppm acetone in the Herriott gas cell and acetone from the NIST database. The correlation coefficient is 0.97.

So, the detection limit is 25 ppb for acetone, 52 ppb for ethanol, 15 ppb for methanol. The transmission spectrum of an acetone mixture in nitrogen with a concentration of 100 ppm was recorded in this work to verify the operability of the developed QCL. The spectrum obtained at the experimental facility is represented in red, and the acetone spectral line from the international NIST database [47] is depicted in black in Figure 6. The Pearson correlation coefficient of the experimental and reference spectra was 0.97.

Conclusion

The paper describes a mid-IR QCL based on a Littrow configuration with an external cavity. The technical characteristics of the developed laser are presented, the design is described, the volt-ampere characteristics are given, as well as the spectral characteristics of the laser. The developed laser has a tuning range 9.6–12.5 μm, maximum peak power 199.8 mW and maximum average power 7.57 mW, tuning step 2 cm^{-1}, spectral width of the laser line 2 cm^{-1}, which makes it possible to solve the problems of absorption spectroscopy and diffuse reflectance spectroscopy with its help.

The paper presents the transmission spectrum of acetone with a concentration of 100 ppm obtained on the experimental setup described in the work, consisting of a QCL, a multi-pass Herriott gas cell with an optical path length of 76 m and two MCT TE photodetectors. The setup can be used to analyze multicomponent gas mixtures, as well as to study human exhaled breath for the presence of biomarker substances for certain diseases. The obtained transmission spectrum is compared with the spectrum from the international database of IR spectra NIST. The correlation coefficient between the spectra was 0.97.

Funding

The study was carried out as part of the implementation of the „Priority-2030“ program of strategic academic leadership approved by the Decree of the Government of the Russian Federation № 729 dated May 13, 2021.

Conflict of interest

The authors declare that they have no conflict of interest.

References

[1] R.F. Kazarinov, R.A. Suris. Sov. Phys. Semicond., **5**, 707 (1971).]
[2] C. Gmachl, F. Capasso, D.L Sivco, A.Y. Cho. Rep. Prog. Phys., **64**, 1533 (2001). DOI: 10.1088/0034-4885/64/11/204
[3] J. Faist, F. Capasso, D.L. Sivco, C. Sirtori, A.L. Hutchinson, A.Y. Cho. Science, **264**, 553 (1994). DOI: 10.1126/science.264.5158.553
[4] F. Capasso. Science, **235**, 172 (1987). DOI: 10.1126/science.235.4785.172
[5] L.A. Skvortsov. *Primenenie kvantovo-kaskadnykh lazerov: sostoyanie i perspektivy* (Technosphere, M., 2020) (in Russian).
[6] S. Slivken, A. Evans, J. David, M. Razeghi. Appl. Phys. Lett., **81**, 4321 (2002). DOI: 10.1063/1.1526462
[7] J. Faist, C. Gmachl, F. Capasso, C. Sirtori, D.L. Sivco, J.N. Baillargeon, A.Y. Cho. Appl. Phys. Lett., **70**, 2670 (1997). DOI: 10.1063/1.119208
[8] R. Maulini, M. Beck, J. Faist, E. Gini. Appl. Phys. Lett., **84**, 1659 (2004). DOI: 10.1063/1.1667609
[9] A. Mendizabal, P.G. Loges. *Proc. SPIE, Optical Fibers and Sensors for Medical Diagnostics, Treatment and Environmental Applications XXIII* (San Francisco, California, United States, 2023), v. 12372, p. 123720H. DOI: 10.1117/12.2655234
[10] P. Kotidis, E.R. Deutsch, A. Goyal. *Proc. SPIE, Micro- and Nanotechnology Sensors, Systems, and Applications VII* (Baltimore, United States, 2015), v. 9467, p. 94672S-1. DOI: 10.1117/12.2178169
[11] I.L. Fufurin, A.S. Tabalina, A.N. Morozov, I.S. Golyak, S.I. Svetlichnyi, D.R. Anfimov, I.V. Kochikov. Opt. Eng., **59** (6), 061621 (2020). DOI: 10.1117/1.OE.59.6.061621
[12] I.S. Golyak, A.N. Morozov, S.I. Svetlichnyi, A.S. Tabalina, I.L. Fufurin. Russ. J. Phys. Chem. B, **13**, 557 (2019). DOI: 0.1134/S1990793119040055
[13] J.R. Castro-Suarez, M. Hidalgo-Santiago, S.P. Hernández-Rivera. Appl. Spectr., **69** (9), 1023 (2015). DOI: 10.1366/14-07626
[14] D.R. Anfimov, I.S. Golyak, O.A. Nebritova, I.L. Fufurin. Russ. J. Phys. Chem. B, **16** (5), 834 (2022). DOI: 10.1134/S1990793122050165
[15] D.A. Samsonov, A.S. Tabalina, I.L. Fufurin. Vestnik of MGTU named after N.E. Bauman. Ser. Estestvennye nauki, **4**, 103 (2018) (in Russian). DOI: 10.18698/1812-3368-2018-4-103-114
[16] D.B. Kelley, D. Wood, A.K. Goyal, P. Kotidis. *Proc. SPIE, Chemical, Biological, Radiological, Nuclear, and Explosives (CBRNE) Sensing XIX* (Orlando, United States, 2018), v. 10629, p. 1062909. DOI: 10.1117/12.2304387

[17] D. Wood, D.B. Kelley, A.K. Goyal, P. Kotidis. *Proc. SPIE, Chemical, Biological, Radiological, Nuclear, and Explosives (CBRNE) Sensing XIX* (Orlando, United States, 2018), v. 10629, p. 1062915. DOI: 10.1117/12.2304453
[18] T. Myers, D. Wood, A.K. Goyal, D. Kelley, P. Kotidis, G. Raz, C. Murphy, C. Georgan. Proc. *SPIE, Algorithms and Technologies for Multispectral, Hyperspectral, and Ultraspectral Imagery XXIII* (Anaheim, United States, 2017), v. 10198, p. 101980C. DOI: 10.1117/12.2262548
[19] A.K. Goyal, D. Wood, V. Lee, J. Rollag, P. Schwarz, L. Zhu, G. Santora. Opt. Eng., **59** (9), 092003 (2020). DOI: 10.1117/1.OE.59.9.092003
[20] A.C. Padilla-Jiménez, W. Ortiz-Rivera, C. Rios-Velazquez, I. Vazquez-Ayala, S.P. Hernández-Rivera. Opt. Eng., **53** (6), 061611 (2014). DOI: 10.1117/1.OE.53.6.061611
[21] K. Yeh, R. Bhargava. *Proc. SPIE, Biomedical Vibrational Spectroscopy* (San Francisco, United States, 2016), v. 9704, p. 970406. DOI: 10.1117/12.2230003
[22] L.L. de Boer, T.M. Bydlon, F. van Duijnhoven, M.T.F.D. Vranken Peeters, C.E. Loo, G.A.O. Winter-Warnars, J. Sanders, H.J.C.M. Sterenborg, B.H.W. Hendriks, T.J.M. Ruers. J. Transl. Med., **16**, 367 (2018). DOI: 10.1186/s12967-018-1747-5
[23] R. Marbach, H.M. Heise. Appl. Opt., **34** (4), 610 (1995). DOI: 10.1364/AO.34.000610
[24] S. Rassel, C. Xu, S. Zhang, D. Ban. Analyst, **145** (7), 2441 (2020). DOI: 10.1039/C9AN02354B
[25] C. Vrancič, N. Kröger, N. Gretz, S. Neudecker, A. Pucci, W. Petrich. Anal. Chem., **86**, 10511 (2014). DOI: 10.1021/ac5028808
[26] J. Haas, E. Vargas Catalán, P. Piron, M. Karlsson, B. Mizaikoff. Analyst, **143**, 5112 (2018). DOI: 10.1039/C8AN00919H
[27] M.J. Norahan, R. Horvath, N. Woitzik, P. Jouy, F. Eigenmann, K. Gerwert, C. Kötting. Anal. Chem., **93**, 6779 (2021). DOI: 10.1021/acs.analchem.1c00666
[28] A. Schwaighofer, B. Lendl. *Vibrational Spectroscopy in Protein Research.* Chapter 3. (Academic Press, Toronto–London–NY., 2020), DOI: 10.1016/B978-0-12-818610-7.00003-7
[29] V.V. Dudelev, D.A. Mikhailov, A.V. Babichev, A.D. Andreev, S.N. Losev, E.A. Kognovitskaya, Yu.K. Bobretsova, S.O. Slipchenko, N.A. Pikhtin, A.G. Gladyshev, D.V. Denisov, I.I. Novikov, L.Ya. Karachinsky, V.I. Kuchinskii, A.Yu. Egorov, G.S. Sokolovskii. Quant. Electron., **50** (2), 141 (2020). DOI: 10.1070/QEL17168
[30] A.V. Babichev, V.V. Dudelev, A.G. Gladyshev, D.A. Mikhailov, A.S. Kurochkin, E.S. Kolodeznyi, V.E. Bougrov, V.N. Nevedomskiy, L.Ya. Karachinsky, I.I. Novikov, D.V. Denisov, A.S. Ionov, S.O. Slipchenko, A.V. Lutetskiy, N.A. Pikhtin, G.S. Sokolovskii, A.Yu. Egorov. Tech. Phys. Lett., **45**, 735 (2019). DOI: 10.1134/S1063785019070174
[31] T. Fei, S. Zhai, J. Zhang, N. Zhuo, J. Liu, L. Wang, S. Liu, Z. Jia, K. Li, Y. Sun, K. Guo, F. Liu, Z. Wang. J. Semicond., **42** (11), 112301 (2021). DOI: 10.1088/1674-4926/42/11/112301
[32] E.R. Deutsch, P. Kotidis, N. Zhu, A.K. Goyal. *Proc. SPIE, Advanced Environmental, Chemical, and Biological Sensing Technologies XI* (Baltimore, United States, 2014), v. 9106, p. 91060A. DOI: 10.1117/12.2058544
[33] I.V. Kochikov, A.N. Morozov, I.L. Fufurin, S.I. Svetlichnyi. Opt. Spectr., **106** (5), 666 (2009). DOI: 10.1134/S0030400X09050075
[34] A.K. Goyal, P. Kotidis, E.R. Deutsch, N. Zhu, M. Norman, J. Ye, K. Zafiriou, A. Mazurenko. *Proc. SPIE, Chemical, Biological, Radiological, Nuclear, and Explosives (CBRNE) Sensing XVI* (Baltimore, United States, 2015), v. 9455, p. 94550L. DOI: 10.1117/12.2177527
[35] A. Reyes-Reyes, Z. Hou, E. van Mastrigt, R.C. Horsten, J.C. de Jongste, M.W. Pijnenburg, H.P. Urbach, N. Bhattacharya. Opt. Express, **22** (15), 18299 (2014). DOI: 10.1364/OE.22.018299
[36] I.S. Golyak, E.R. Kareva, I.L. Fufurin, D.R. Fufurin, A.V. Shcherbakova, O.A. Nebritova, P.P. Demkin, A.N. Morozov. Komp'yuternaya optika, **46** (4), 650 (2022) (in Russian). DOI: 10.18287/2412-6179-CO-1058
[37] A. Genner, P. Martín-Mateos, H. Moser, B. Lendl. Sensors, **20**, 1850 (2020). DOI: 10.3390/s20071850
[38] F. Zheng, X. Qiu, L. Shao, S. Feng, T. Cheng, X. He, Q. He, C. Li, R. Kan, C. Fittschen. Opt. Laser Technol., **124**, 105963 (2020). DOI: 10.1016/j.optlastec.2019.105963
[39] N. Liu, L. Xu, S. Zhou, L. Zhang, J. Li. Analyst, **146**, 3841 (2021). DOI: 10.1039/C9AN02354B
[40] X. Tian, F. Beén, P.S. Bäuerlein. Environmental Research, **212** (D), 113569 (2022). DOI: 10.1016/j.envres.2022.113569
[41] A. Reyes-Reyes, R.C. Horsten, H.P. Urbach, N. Bhattacharya. Analyt. Chem., **87** (1), 507 (2015). DOI: 10.1021/ac504235e
[42] A.V. Shcherbakova, D.R. Anfimov, I.L. Fufurin, I.S. Golyak, I.A. Trapeznikova, E.R. Kareva, A.N. Morozov. Opt. Spectr., **129** (6), 830 (2021). DOI: 10.1134/S0030400X21060151
[43] O.A. Nebritova, P.P. Demkin, A.N. Morozov, P.V. Berezhansky, D.R. Anfimov, I.L. Fufurin. Vestnik of MGTU named after N.E. Bauman. Ser. Yestestvennyye nauki, **6**, 39 (2023) (in Russian). DOI: 10.18698/1812-3368-2023-6-39-54
[44] I. Fufurin, P. Berezhanskiy, I. Golyak, D. Anfimov, E. Kareva, A. Scherbakova, P. Demkin, O. Nebritova, A. Morozov. Materials, **15**, 2984 (2022). DOI: 10.3390/ma15092984
[45] I.S. Golyak, P.V. Berezhansky, A.Yu. Sedova, T.A. Gutyrchik, O.A. Nebritova, A.N. Morozov, D.R. Anfimov, I.B. Vintaikin, A.A. Konopleva, P.P. Demkin, I.L. Fufurin. Opt. i spektr., **131** (6), 825 (2023) (in Russian). DOI: 10.21883/OS.2023.06.55917.109-23
[46] I.L. Fufurin, D.R. Anfimov, E.R. Kareva, A.V. Scherbakova, P.P. Demkin, A.N. Morozov, I.S. Golyak. Opt. Eng., **60** (8), 082016 (2021). DOI: 10.1117/1.OE.60.8.082016
[47] *NIST Chemistry WebBook.* [Electronic resource]. 1996. Date of update: 01.2023. URL: https://webbook.nist.gov/chemistry/ (date of application: 29.12.2023). DOI: 10.18434/T4D303

Translated by A.Akhtyamov